ISSN: 0975-833X

Available online at http://www.journalcra.com

International Journal of Current Research
Vol. 8, Issue, 03, pp. 27993-27999, March, 2016

INTERNATIONAL JOURNAL OF CURRENT RESEARCH

RESEARCH ARTICLE

CURCUMIN LOADED HAp@SiO_2 CORE-SHELL NPs AS A CARRIER FOR TARGETED DRUG DELIVERY IN THE TREATMENT OF CANCER

Ramesh, I. and *Meena, K. S.

Research Scholar, Department of Chemistry, Queen Mary's College, Chennai, Tamilnadu, India

ARTICLE INFO

Article History:
Received 20th December, 2015
Received in revised form
16th January, 2016
Accepted 24th February, 2016
Published online 16th March, 2016

Key words:
Ceramic NPs,
Curcumin,
Targeted drug delivery,
Biotin receptors.

ABSTRACT

We are developed the targeted drug delivery by HAp@SiO_2 core-shell NPs. Hydroxyapatite (HAp) core was prepared by wet chemical co-precipitation method using different chemical precursors and silica shell coated on the HAp nanoparticle by stober's process. Polyethylene glycol and biotin was functionalized with HAp@SiO_2 core-shell NPs via covalent linkage. curcumin was loaded onto the surface of HAp@SiO_2 core-shell NPs by the electrostatic interaction between curcumin molecules and the polymer segment. HAp@SiO_2 core-shell NPs was characterized by UV-visible, XRD, HR-TEM, and the polyethylene glycol (PEG), biotin conjugation was confirmed by FT-IR techniques. The drug release behaviour of HAp@SiO_2-PEG-biotin NPs was investigated at different pH condition (PBS, pH-7.4 and 6.0).The cytotoxicity of the core-shell NPs against MCF-7(receptor-positive) and NIH-3T3 (receptor-negative) cell lines was assessed using the MTT assay. The results showed that curcumin loaded NPs increased cytotoxicity effect in MCF-7 than NIH-3T3 cell line. The overall results shown that the biocompatible HAp@SiO_2 core-shell NPs may be a suitable nanocarrier for targeted drug delivery system.

Citation: Ramesh, I. and Meena, K. S. 2016. "Curcumin loaded HAp@SiO_2 core-shell NPs as a carrier for targeted drug delivery in the treatment of cancer", *International Journal of Current Research,* 8, (03), 27993-27999.

INTRODUCTION

Curcumin (CUR) is a widely known natural bioactive polyphenolic component of turmeric. Curcuminis also a "Generally Recognized As Safe" compound by the Food and Drug Administration (U.S. Food and Drug Administration, 2012). Curcumin is one of the most promising natural anticancer agents and hence been much investigated for the past few decades (Bar-Sela *et al*., 2010; Yallapu *et al*., 2012), but it has not yet been approved as a therapeutic agent; because its poor absorption, permeability, rapid metabolism, and elimination of curcumin in turn leading to poor oral bioavailability, and lack of cancer cell targeting. However, poor oral bioavailability of curcumin is mainly due to its poor aqueous solubility, these limitations can be overcome by nanoparticulate drug delivery system, by the synthesis of adjuvant which can block the metabolic pathways of curcumin, design of NPs complexes have been made to provide longer circulation, better permeability, and resistance to metabolic processes (Shoba *et al*., 1998; Cruz-Correa *et al*., 2006; Verma *et al*., 1997; Li *et al*., 2005; Maiti *et al*., 2007; Suresh and Srinivasan, 2007). Though nanoparticle based drug delivery systems provide a suitable solution to circumvent the solubility problems of highly hydrophobic drug like curcumin, very few studies have been published citing curcumin NPs. Curcumin act as an effective chemotherapy agent against caancer cell lines by reported in the literature (Bisht *et al*., 2007). In recent decades, the production of bioceramic NPs has attracted much attention for biomedical application.

Hydroxyapatite ($Ca_{10}(PO_4)_6(OH)_2$) (HAp), which is the major inorganic component of bone and teeth, is a key biomaterial because of its excellent biocompatibility, bioactivity, and osteocoductivity (Sandra *et al*., 2013; Li *et al*., 2013). HAp has achieved excellent results as bioceramics in bone-substituted operations and in teeth repair due to its unique mechanical properties and bioactivity (Capriotti *et al*., 2007; Zhou and Lee, 2011). Moreover, owing to its nontoxicity and non inflammatory properties, it has great potential application in drug storage/ release system (Zhang *et al*., 2010). As an effective drug carrier, a high drug loading capacity is necessary (Climent *et al*., 2009; Jurgons *et al*., 2006). However, the low surface area of HAp may limit its further application in many conditions. Silica is still considered to be the best candidate for surface functionalization because due its good biocompatibility in human body and high specific surface area (high drug loading capacity) it is highly stable against degradation.

Corresponding author: Meena, K. S.
Department of Chemistry, Queen Mary's College, Chennai, Tamilnadu, India.

Furthermore, silica act to improve the biocompatibility, hydrophilicity as well as the surface functionality due to the availability of abundant silanol groups (-SiOH) on the surface (Raco *et al*., 2012). Therefore, synthesis of silica coated HAp nano-sized core-shell structure with larger surface area should be able to reach this goal. The core-shell composite structures, as a kind of new nanostructures, have received intense attention due to their improved physical and chemical properties over their single components, and thus many efforts have been made to synthesize such special core-shell nanostructures (Ahmed *et al*., 2006; Bonini *et al*., 2006). Polyethylene glycol is used to targeted drug delivery system because it is non-toxic, non-immunogenic, and non-antigenic. It is coated on the NPs surface to disperse it, to reduced the non-specific protein adsorption and clearance by macrophages and to render the NPs capable of crossing the cell membrane. PEG prevents the NPs from agglomeration, prevent particle surface from oxidation and make them more biocompatible. The major advantage of PEG coating is that it increases the circulation time because of resistance to plasma protein deposition (Brigger *et al*., 2002; Hubbell, 2003; Riess, 2003). At present, targeted drug delivery ("Active targeting") is used to describe specific interactions between drug/drug carrier and the target cells, usually through specific ligand-receptor interactions (Beduneau *et al*., 2007; Deckert, 2009; Hong *et al*., 2009; Zensi *et al*., 2009; Canal *et al*., 2010). Though cancerous tumors exhibit higher biotin content than normal tissue, few studies have analyzed drug delivery systems using vitamin H (biotin) as a ligand for cancer targeting. Interestingly, one study illustrated that in the over-expression of either folate or vitamin B_{12} receptors, there is also an extreme increase in the expression of biotin receptors. Biotin receptors have been found to be highly active and over expressed in different cancer cells (Vadlapudi *et al*., 2013; Soininen *et al*., 2012).

In this paper, synthesis and characterization of curcumin loaded HAp@SiO_2-PEG-biotin NPs as a carrier for targeted drug delivery in the treatment of cancer. The structure of core-shell NPs was characterized by fourier transform infrared (FTIR), X-ray diffraction (XRD), and high resolution transmission electron microscopy (HRTEM) techniques. The in vitro drug release was performed at different pH codition (pH-7.4 and 6.0). The cytotoxicity of the core-shell NPs against human breast cancer cell line (MCF-7) and fibroblast (NIH-3T3) cell lines were assessed using the MTT assay.

MATERIALS AND METHODS

Chemicals

Calciumnitrate tetrahydrate $Ca(NO_3)_2$ $4H_2O$, Diammonium hydrogen phosphate $(NH_4)_2HPO_4$, Tetraethylorthosilicate (TEOS), polyethylene glycole (HOOC-PEG-NH_2) (MW-2100), Biotin, Curcumin, were purchased from Sigma Chemicals (USA). All the other chemicals used were of analytical grade. Mill-Q water was used for all the experiments.

Synthesis of HAp NPs

The HAp NPs was prepared by slight modification of the method described in the literature (Bouyer *et al*., 2000). Briefly, 1 M of $Ca(NO_3)_2$ $4H_2O$ and 0.6 M of $(NH_4)_2HPO_4$ were dissolved in Milli-Q water separately. The pH of both aqueous solutions was brought to 11 by using 25% of NH_4OH solution under vigorous stirring the $Ca(NO_3)_2$ $4H_2O$ was added drop wise to $(NH_4)_2HPO_4$ solution over a period of 1 h to produce a milky white precipitate, which was then stirred for 1 h. Then the reflux process was carried out at 100 ^{0}C for 1 h followed by aging for 24 h. Finally, the obtained product was washed with distilled water, centrifuged and dried at 100 ^{0}C for 12 h and then calcined at 400 ^{0}C for 3 h.

Synthesis of HAp@SiO_2 core-shell NPs

Silica-coating procedure based on the stober process (Stober *et al*., 1968), was carried out to encapsulate HAp NPs. Initially, 50 mg of HAp NPs were dispersed in 60 ml of ethanol by sonication for 30 min to ensure complete dispersion and then 0.6 ml of tetraethylorthosilicate (TEOS) was added to the above suspension to carry out the silica growth. The HAp@TEOS was allowed to stir for 30 min, thereafter ammonium hydroxide was added in a 1:4 TEOS to NH_4OH volume ratio. The mixture was stirred for 24 h to ensure the completion of reaction. Finally, the obtained precipitate was separated by centrifugation and washed with ethanol to remove the secondary silica particles.

Synthesis of amine coated HAp@SiO_2 core-shell NPs

The amine functionalized HAp@SiO_2 core-shell NPs was prepared by slight modification of the technique described in the literature (Ma *et al*., 2003). First, 30 mg of HAp@SiO_2 core-shell NPs was added to 60 ml of toluene and stirred for 6 h before adding 1.0 ml 3-amino propyl trimethoxy silane (APTES). After stirring at room temperature for 24 h, the amine functionalized NPs were separated by centrifugation was washed with toluene and dried in a fume-hood at room temperature.

Synthesis of PEG conjugated HAp@SiO_2 core-shell NPs

Polyethylene glycol was covalently linked to the HAp@SiO_2-NH_2 NPs via EDAC/NHS method as follows. 0.3 g of PEG (0.15 mm) was dissolved in alkaline Milli-Q water. To this 0.057 g of EDC (0.30 mm) and 0.034 g of NHS (0.30 mm) were added and the pH of the resulting solution was kept at 7.0-8.0 with 0.5 ml of TEA. The activation was carried at room temperature for 3 h. Then 0.1 g of aqueous dispersed aminated NPs was added drop wise to the activated polymer solution and the whole solution was stirred for 24 h at room temperature to form polymer modified HAp@SiO_2 NPs was separated by centrifugation and washed with Milli-Q water for several times and dried at 60 ^{0}C for 12 h.

Synthesis of biotin functionalized HAp@SiO_2-PEG NPs

In brief, 36 mg biotin (0.15 mm) was dissolved in 10 ml DMSO-Milli-Q water, and the pH was maintained ~8.0 by 0.5 ml of TEA. To the above biotin solution, EDC (57 mg, 0.30 mm) and NHS (34 mg, 0.30 mm) were added and pH of the mixture was maintained 7.0-8.0 by 0.5 ml of TEA. The biotin activation was carried out for 4 hrs under dark condition at room temperature. Thereafter, 50 mg of aqueous dispersion of

HAp@SiO_2-PEG core-shell NPs was added drop wise to the activated biotin solution, and the resulting mixture was stirred for overnight in the dark at room temperature. Finally, the biotin-modified HAp@SiO_2-PEG was precipitated by centrifugation and washed with water and DMSO several times and dried in vacuum at 60 ^{0}C for 12 h.

Encapsulation of curcumin onto HAp@SiO_2-PEG-biotin NPs

5 mg of curcumin was dissolved in 5 ml of acetone and then 10 mg of HAp@SiO_2-PEG-biotin NPs was added in to curcumin solution, the solution was stirred at room temperature for 4 h, free drug was separated from the encapsulated drug using centrifugation.

Drug loading and entrapment efficacy

In addition, the drug loading content and entrapment efficacy was determined by the following equation:

$$\text{Drug loading contents (\%)} = \frac{\text{Weight of drug in NPs}}{\text{Weight of NPs taken}} \times 100$$

$$\text{Drug entrapment efficacy (\%)} = \frac{\text{Weight of drug in NPs}}{\text{Weight of drug taken}} \times 100$$

In-vitro drug release

In order to determine the drug release pro le of the curcumin loaded HAp@SiO_2-PEG-biotin NPs was introduced into a screw capped glass bottle containing 50 ml of phosphate buffered saline (PBS, pH-7.4 and 6.0) medium at 37 °C and pH 7.4 under sterile condition. 5 ml samples were withdrawn by a pipette at a regular interval of 1 h and replaced immediately with 5 ml of fresh PBS medium, which was accounted for when calculating the amount released. Drug concentration in the collected samples was measured UV spectrophotometer at a wavelength of 450 nm.

Cell viability studies

The MTT assay is based on the ability of live but not dead cells to reduce a yellow tetrazolium dye to a purple formazan product. Cells were maintained in DMEM medium, supplemented with 10% Fetal Bovine Serum, at 37^{o}C in humidified atmosphere with 5% CO_2. The cells were plated in 96 well flat bottom tissue culture plates at a density of approximately 1.2X 10^4 cells/well and allowed to attach overnight at 37^{o}C. The medium was then discarded and cells were incubated with different concentrations of the samples (10, 20, 30, 40, 50, 60 µg/ml) for 24 hours. After the incubation, medium was discarded and 100µl fresh medium was added with 10µl of MTT (5mg/ml). After 4 hours, the medium was discarded and 100µl of DMSO was added to dissolve the formazan crystals. Then, the absorbance was read at 570 nm in a microtitre plate reader (Mossman, 1983).

Cell survival was calculated by the following formula:

Viability % = (Test OD/ Control OD) X 100
Cytotoxicity % = 100 – Viability%

Characterization

Characterization of NPs

Fourier transform infrared (FT-IR) spectra was measured on FTIR spectrometer (Bruker IFS 55, Fallanden, Switzerland), X-ray diffraction (XRD) patterns were taken from X'pert PRO PAN alytical diffractometer operating with CuKα (radiation (λ=1.5406A°) source, and high resolution transmission electron microscopy (HRTEM) photographs were taken using a JEOL JEM -3010 Electron microscope operating at 300 keV, the magnifying power used was 600 and 800k times.

RESULTS AND DISCUSSION

FT-IR spectra analysis

Fig.(1a & 1b) shows the FTIR spectra of HAp@SiO_2-NH_2 and HAp@SiO_2-PEG-biotin NPs respectively. The characteristic peaks for PO_4^{3-} appear at around 565, 950, and 601 cm^{-1}. The peaks at 1,000–1,250 cm^{-1} corresponds the asymmetric and symmetric vibrations of Si–O–Si (Pasternack *et al*., 2008). The band at 1633 cm^{-1} is assigned to N-H bend. This peak could be attributed to the amine group was successfully functionalized surface on the HAp@SiO_2 NPs, and the additional peak at 3421 cm^{-1} was assigned both –NH_2 and H_2O group of amine functionalized NPS. The FTIR spectrum of HAp@SiO_2-PEG-biotin NPs was shown in Fig-1(b). The peak at 2,927 cm^{-1}, was assigned to the CH_2 stretching of PEG, the biotin conjugated HAp@SiO_2-PEG particles demonstrated at 1540 cm^{-1}, and 1680 cm^{-1}, assigned to the amide II (N-H bend + C-N stretch) and amide I (C=O stretch) vibrational modes respectively and indicate the amide bond formed between biotin and the surface of the HAp@SiO_2-PEG NPs (Socrates, 2001).

XRD analysis

The XRD pattern of the as prepared HAp nanoparticle is shown in the Fig.2 (a). After calcination, the powders reveal the crystallinity con rmation of $Ca_{10}(PO_4)_6(OH)_2$ (HAp), and can be well indexed to hexagonal crystal structure, ICDD(PDF Card le no. 9-432). According to Scherrer's formula, the diameter of the crystalline grain.

$D = 0.9\lambda / (\beta\cos\theta)$

Where, β, λ and θ is full width at half maximum (FWHM) of the intensity, incident wavelength (for Cu(kα), λ= 1.54056 A˚) and re ection angle, respectively. The average crystallite size estimated from the XRD line broadening is around 21 nm (Hamadouche and Sedel, 2000). For silica coated HAp nanoparticles as seen in Fig.2 (b). Peaks for HAp are not clearly seen due to suppressed by amorphous silica. This result indicated that the silica coating is thick to completely mask the HAp peaks and the shell thickness in the range of 17 nm. The suppression is more remarkable with the introduction of higher silica content.

HR-TEM

The HR-TEM image of HAp NPs shown in Fig.3 (a) the image indicated that the as-synthesized HAp powders was mono-dispersive and had a smooth surface and a rod-like shape, and the particle of diameter in the range of 21 nm were observed.

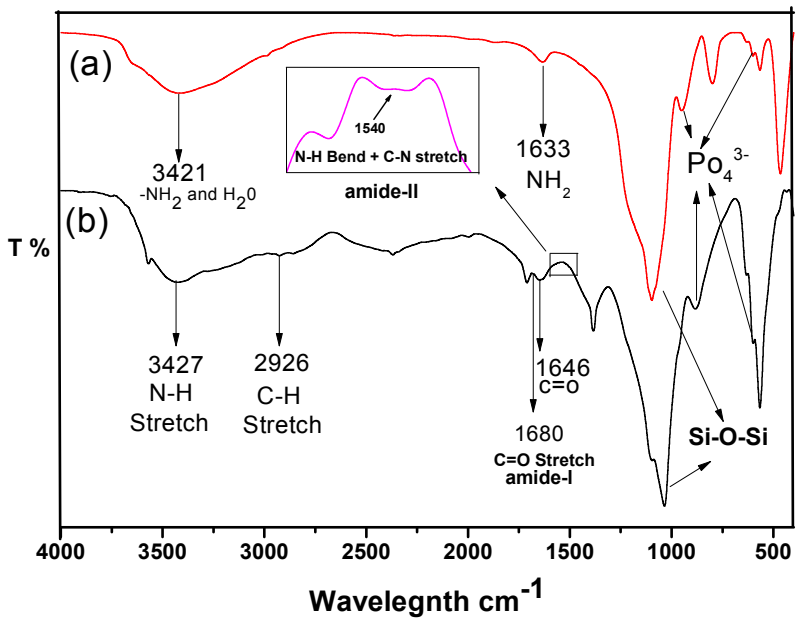

Fig.1. FTIR spectra of (a) HAp@SiO_2-NH_2 (b) HAp@SiO_2-PEG-biotin NPs

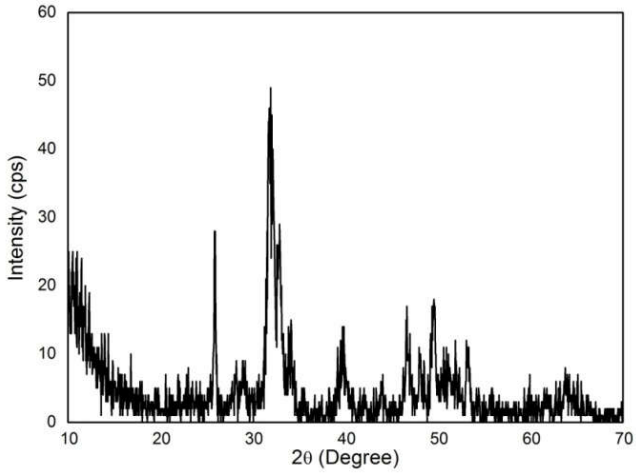

Fig.2. (a) XRD Pattern of HAp NPs

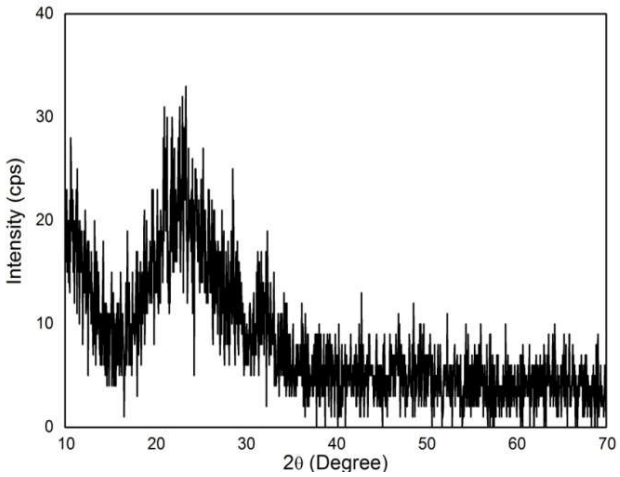

Fig.2. (b) XRD Pattern of HAp@SiO_2 NPs

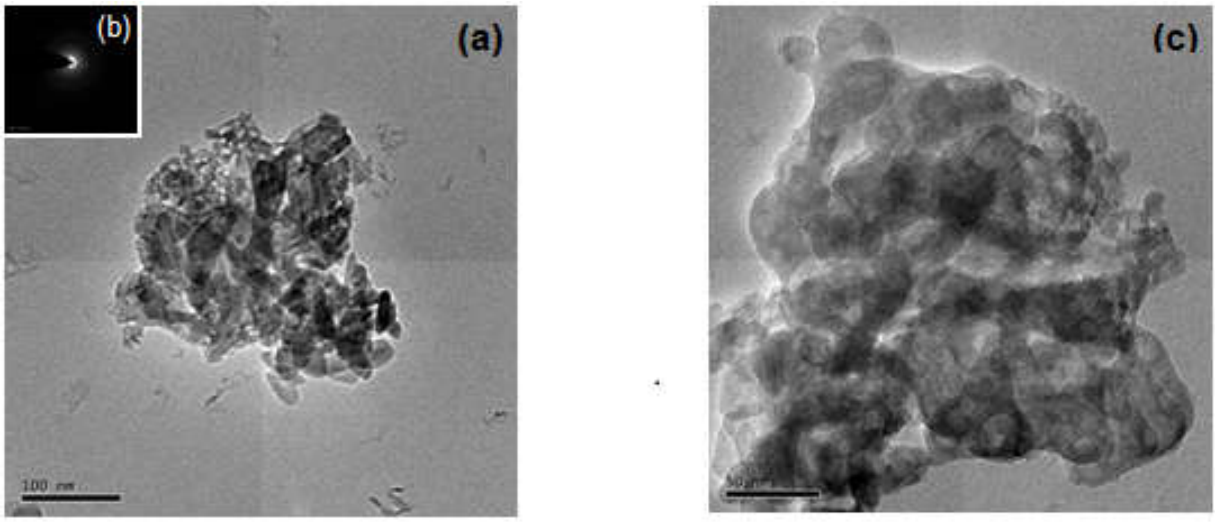

Fig.3. HR-TEM images of (a) HAp (b) SEAD image of HAp (c) HAp@SiO_2 NPs

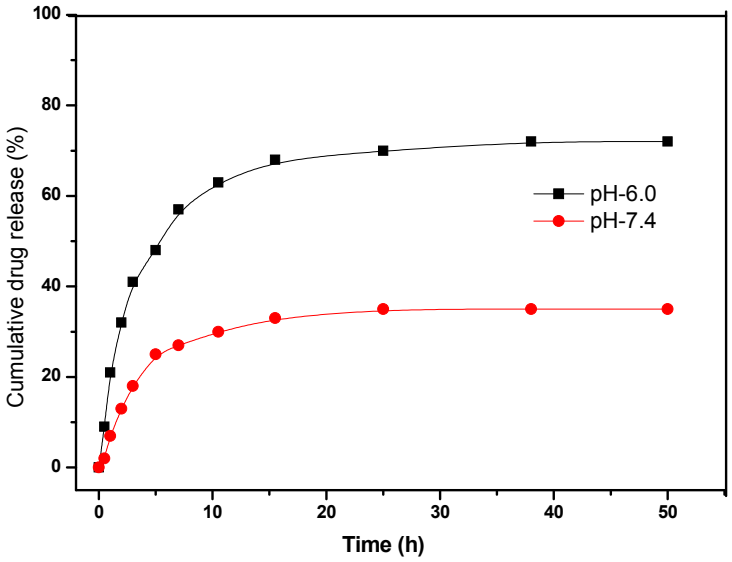

Fig.4. In vitro drug release profile of HAp@SiO_2-PEG-biotin core-shell Nps

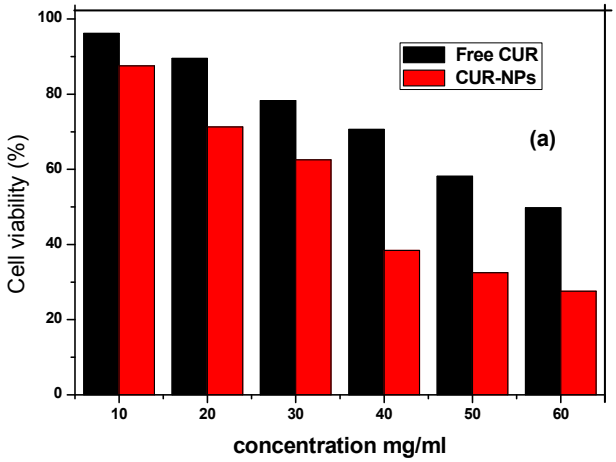

Fig.5(a). In-vitro cytotoxicity effect of HAp@SiO_2-PEG-biotin core-shell NPs against MCF-7 cell line

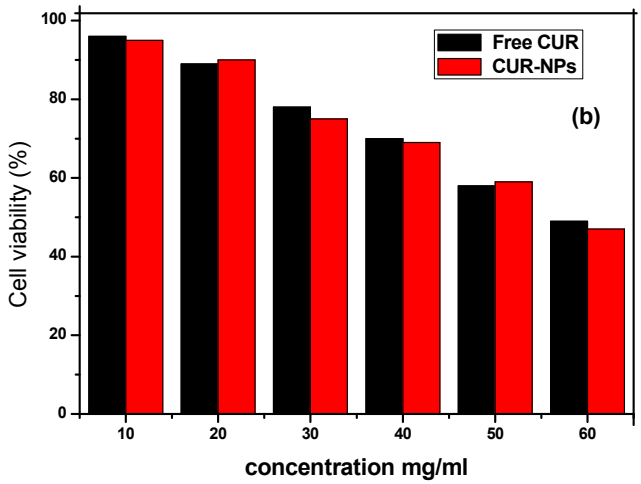

Fig.5(b). In-vitro cytotoxicity effect of HAp@SiO_2-PEG-biotin core-shell NPs against NIH-3T3 cell line

The crystalline structure of the HAp NPs was further confirmed by selected-area electron diffraction (SAED) image investigations in (Fig-3b). The transmission electron microscopic analysis was carried out to con rmed the particle size, growth pattern and distribution of crystallites. The core–shell structure image of HAp@SiO_2 particles clearly displays in (Fig-3c). A nearly well de ned spherical morphology is observed and all the HAp particles appear to be associated within SiO_2 shell. The boundary between the core HAp and the shell SiO_2 is very much distinct. The core-shell particle size diameter is nearly 35 nm.

In-vitro drug release

In-vitro drug release profile of curcumin loaded HAp@SiO_2-PEG-biotin is shown in Fig.4. The loading of CUR into the HAp@SiO_2 NPs via electrostatic interaction between curcumin and polymer segment. The loading content and entrapment efficiency of cucumin in HAp@SiO_2-PEG-biotin NPs are found to be 27.2% and 78.4% respectively. Further, the amount of CUR released from the HAp@SiO_2-PEG-biotin NPs was investigated at different pH (7.4, and 6.0) showed in Fig-4. Drug release profile shows 30% and 76% release of CUR in 50 h at pH-7.4, and 6.0 respectively. The drug is released gradually over a period of time. This shows that the drug is released in a sustained manner. In the initial stage there is a rapid release of drug. It corresponds to the drug molecules present close to the surface. It is followed by a slow and steady release of drug that is strongly bound to the polymer and is released from below the surface. The drug release at pH-6.0 was greater than pH-7.4 due to the protanation of polymer segment which cause the drug-polymer interaction became weak and as a result CUR gets released at a much faster rate and in larger amount. Therefore, the drug release behaviour of HAp@SiO_2-PEG-biotin NPs may benefit the tumor treatment.

Cytotoxicity test

The cytotoxicity of the HAp@SiO_2-PEG-biotin NPs was determined in the MCF-7 and NIH-3T3 cell lines using the MTT assay shown in Fig.5 (a & b) respectively. The MTT assay is based on the ability of a mitochondrial dehydrogenation enzyme in viable cells to cleave the tetrazolium rings of the pale yellow MTT and form purple formazan crystals (Mossman, 1983). Therefore, the number of surviving cells is directly proportionate to the level of the formed Formazan. The cytotoxicity profile MCF-7 and NIH-3T3 cells were incubated with different concentrations (10, 20, 30, 40, 50, 60 µg/ml) of the free CUR, and CUR loaded HAp@SiO_2-PEG-biotin NPs for 24 hours.There was no significant difference in cell viability incubation with curcumin between MCF-7 and NIH-3T3 cells lines. The cytotoxicity of NIH-3T3 cells after incubation with CUR loaded HAp@SiO_2-PEG-biotin NPs for 24 h at the concentrations of 50 and 60 µg/ml was 59% and 48%, respectively. In contrast, the cytotoxicity of MCF-7 cells incubation with the same concentration of former NPs increased to 32% and 27%, respectively. This increased cytotoxicity of HAp@SiO_2-PEG-biotin against MCF-7 could be explained by the improved cellular uptake of HAp@SiO_2-PEG-biotin NPs via biotin receptor-mediated endocytosis.

Conclusion

In summary, synthesized and characterized of curcumin loaded HAp@SiO_2 core-shell NPs was developed for tumor targeted drug delivery. The HAp and HAp@SiO_2 NPs of diameter was observed in the range of 21 and 35 nm respectively. This is in desired size-range for drug delivery application. PEG and biotin conjugated onto the surface of the HAp@SiO_2 core-shell NPs was explained by FTIR Spectroscopy analysis. The loading of curcumin into the HAp@SiO_2-PEG-biotin NPs is due to the electrostatic interaction between curcumin molecules and the Polymer segment. Curcumin loading content and entrapment efficiency was reached high as 27.2% and 78.4% respectively. The drug release profile of curcumin from biotin modified PEG functionalized HAp@SiO_2 core-shell NPs were investigated at different pH (PBS, pH 7.4, and 6.0). Curcumin release profile of PEG-biotin conjugated HAp@SiO_2 NPs were showed that up to 76% of adsorbed drug was released in 50 h. The cytotoxicity of the curcumin loaded HAp@SiO_2-PEG-biotin NPs was determined in the MCF-7 and NIH-3T3 cell lines via biotin receptor-mediated endocytosis, using the MTT assay. The results showed that curcumin loaded NPs increased cytotoxicity effect in MCF-7 than receptor-negative NIH-3T3 cell lines. These overall results demonstrate that our HAp@SiO_2-PEG-biotin core-shell NPs is a promising for biotin receptor-mediated tumor-targeted drug delivery in upcoming decades.

REFERENCES

Ahmed M.E., Y. Shu, S. Tsugio, 2006. Control of silica shell thickness and microporosity of titania–silica core–shell type nanoparticles to depress the photocatalytic activity of titania, *J. Colloid Interface Sci*., 300, 123.

Albumin nanoparticles targeted with ApoE enter the CNS by transcytosis and are delivered to neurons, *J. Control. Release*, 137, 78–86.

Bar-Sela G, Epelbaum R, Schaffer M. 2010. Curcumin as an anti-cancer agent: review of the gap between basic and clinical applications. *Curr Med Chem*., 17:190–197.

Beduneau A., P. Saulnier, F. Hindre, A. Clavreul, J.C. Leroux, J.P. Benoit, 2007. Design of targeted lipid nanocapsules by conjugation of whole antibodies and antibody Fab' fragments, *Biomaterials,* 28, 4978–4990.

Bisht S., G. Feldmann, S. Soni, R. Ravi, C. Karikar, A. Maitra, and A. Maitra, 2007. Polymeric nanoparticle-encapsulated curcumin ("nanocurcumin"): A novel strategy for human cancer therapy. *J. Nanobiotechnol*., 5, 1.

Bonini M., A. Wiedenmann, P. Baglioni, Synthesis and characterization of magnetic nanoparticles coated with a uniform silica shell. 2006. *Mater. Sci.Eng*., C26, 745.

Bouyer E, Gitzhofer F, Boulos MI. Morphological study of hydroxyapatite nanocrystal suspension. *J Mater Sci Mater Med*., 2000; 11: 523-31.

Brigger I., C. Dubernet, and P. Couvreur, Nanoparticles in cancer therapy and diagnosis. 2002. *Adv. Drug Deliver. Rev*., 54, 631.

Canal F., M.J. Vicent, G. Pasut, O. 2010. Schiavon, Relevance of folic acid/polymer ratio in targeted PEG-epirubicin conjugates, *J. Control. Release*, 146, 388–399.

Capriotti L. A., T. P. Beebe and J. P. Schneider, 2007. Hydroxyapatite surface-induced peptide folding. *J. Am.Chem. Soc*., 129, 5281–5287.

Chen H., B.H. Clarkson, K. Sun, J.F. 2005. Mansfield, Selfassembly of synthetic hydroxyapatite nanorods into an enamel prism-like structure. *J. Colloid Interface Sci*., 288, 97-103.

Climent E., A. Bernardos, M. R. Martinea, A. Maquieira, M. D.Marcos, N. N. Pastor and R. Puchades, Controlled Delivery Systems Using Antibody-Capped Mesoporous Nanocontainers. *J. Am. Chem. Soc*., 2009, 131, 14075–14080.

Cruz-Correa M., D. A. Shoskes, P. Sanchez, R. Zhao, L. M. Hylind, S. D. Wexner, and F. M. Giardiello, 2006. Combination treatment with curcumin and quercetin of adenomas in familial adenomatous polyposis. *Clin. Gastroenterol. Hepatol*., 4, 1035.

Deckert P.M., Current constructs and targets in clinical development for antibodybased cancer therapy, *Current Drug Targets*, 10 (2009) 158–175.

Hamadouche, M.; Sedel, L. Ceramics in orthopaedics. J. Bone Jt. Surg. Br. 2000, 82, 1095–1099.

Hong M., S. Zhu, Y. Jiang, G. Tang, Y. Pei, Efficient tumor targeting of hydroxycamptothecin loaded PEGylated niosomes modified with transferrin, *J. Control. Release*, 133 (2009) 96–102.

Hubbell, J. A. 2003. Enhancing drug function, Science, 300,595.

Jurgons R., C. Seliger, A. Hilpert, L. Trahms, S. Odenbach and C. J. Alexiou, 2006. Drug loaded magnetic nanoparticles for cancer therapy. *Phys. Condens. Matter*., 18, 2893–2902.

Li L., F. S. Braiteh, and R. Kurzrock, 2005. Liposomeencapsulated curcumin: in vitro and in vivo effects on proliferation, apoptosis, signaling, and angiogenesis. *Cancer*, 104, 1322.

Li M., Y. B. Wang, Q. Liu, Q. H. Li, Y. Cheng, Y. F. Zheng, T. F. Xi and S. C. Wei, In situ synthesis and biocompatibility of nano hydroxyapatite on pristine and chitosanfunctionalized graphene oxide. *J. Mater. Chem. B*, 2013, 1, 475–484.

Lin K., J. Chang, R. Cheng, M. Ruan, 2007. Hydrothermal microemulsion synthesis of stoichiometric single crystal hydroxyapatite nanorods with mono-dispersion and narrowsize distribution, *Mater. Lett*., 61, 1683–1687.

Ma M. *et al*. 2003. Colloids and Surfaces A: Physicochem. Eng. Aspects 212, 219-226.

Maiti K., K. Mukherjee, A. Gantait, B. Pada Saha, and P. K. 2007. Mukherjee, Curcumin–phospholipid complex: Preparation, therapeutic evaluation and pharmacokinetic study in rats. *Int. J. Pharm*., 330, 155163.

Mossman, T. 1983. Rapid colorimetric assay for cellular growth and survival – application to proliferation and cytotoxicity assays. *J.Immunol.Methods*, 65: 55-63.

Pasternack RM, Rivillon-Amy S, Chabal YJ. 2008. Attachment of 3–(aminopropyl) triethoxysilane on silicon oxide surfaces: Dependence on solution temperature. Langmuir 24:12963–12971.(*PubMed*: 18942864)

Raco AG, Carmona D, Migulel-Sancho N, Bomati- Migulel O, Balas F, *et al*. 2012. Surface functionalization for tailoring the aggregation and magnetic behaviour of silica-coated iron oxide nanostructures. *Nanotechnology*, 23:155603.

Riess, G. 2003. Micellization of block copolymers, *Prog. Polym. Sci*., 28, 1107.

Sandra S. S., C. Montserrat, I. B. Isable and V. R. Maria, Design and preparation of biocompatible zwitterionic hydroxyapatite, *J. Mater. Chem., B*, 2013, 1,1595–1606.

Shoba G., D. Joy, T. Joseph, M. Majeed, R. Rajendran, and P.S.Srinivas, 1998. Influence of piperine on the pharmacokinetics of curcumin in animals and human volunteers. *Planta Med*., 64, 353.

Socrates, G. 2001. Infrared and Raman Characteristic Group Frequencies - Tables and Charts. 3. John Wiley & Sons Ltd;West Sussex, England.

Soininen S.K.; Lehtolainen-Dalkilic P.; Karppinen T.;Puustinen T.; Dragneva G.; Kaikkonen M.U.; Jauhiainen M.; Allart B.; Selwood D.L.; Wirth T.; Lesch H.P.; Määttä A.M.; Mönkkönen J.; Ylä-Herttuala S.; Ruponen M. 2012.

Stober W., A. Fink, E. Bohn, 1968. Controlled growth of monodisperse silica spheres in the micron size range, *J.Colloid Interf. Sci*., 26, 62–66.

Sun Y., G. Guo, Z. Wang, H. Guo, 2006. Synthesis of singlecrystal HAP nanorods Ceram. *Int*. 32, 951–954.

Suresh D. and K. Srinivasan, 2007. Studies on the in vitro absorption of spice principles-Curcumin, capsaicin and piperine in rat intestines. *Food Chem. Toxicol*., 45, 1437.

Targeted delivery via avidin fusion protein: intracellular fate of biotinylated doxorubicin derivative and cellular uptake kinetics and biodistribution of biotinylated liposomes. *Eur. J. Pharm. Sci*., 47, 848-856.

U.S. Food and Drug Administration. Food additive status list. Revised as of April 1. (Assed on july17,2012.) http://www.accessdata.fda.gov/scripts/cdrh/cfcfr/CFRSearch. cfm?fr=182.20.

Vadlapudi A.D.; Vadlapatla R-K.; Pal D.; Mitra A.K. 2013.Biotin uptake by T47D breast cancer cells: functional and molecular evidence of sodium-dependent multivitamin transporter (SMVT). *Int. J. Pharm*., 441, 535-543.

Verma S. P., E. Salamone, and B. Goldin, 1997. Curcumin and genistein, plant natural products, show synergistic inhibitory effects on the growth of human breast cancer MCF-7 cells induced by estrogenic pesticides. *Biochem. Biophys. Res. Commun*., 233, 692.

Yallapu MM, Jaggi M, Chauhan SC: 2012. Curcumin nanoformulations: a future nanomedicine for cancer. *Drug Discov*., Today 17(1–2):71–80.

Yang Chun., Guo Ying-kui., Zhang Mi-lin, Thermal decomposition and mechanical properties of hydroxyapatite ceramic. *Trans. Nonferrous Met. Soc. China*, 20(2010)254 258

Zensi A., D. Begley, C. Pontikis, C. Legros, L. Mihoreanu, S. Wagner, C. Büchel, H.v. Briesen, J. Kreuter, 2009.

Zhang C., C. Li, S. Huang, Z. Hou, Z. Cheng, P. Yang, C. Peng and J. Lin, Self-activated luminescent and mesoporous strontium hydroxyapatite nanorods for drug deliver. *Biomaterials*, 2010, 31, 3374–3383.

****